Kinetic Multiscale Modeling and Simulation of Cluster Formation Processes in Free Gas Expansions Using DSMC

Deborah A. Levin[*†] and Jiaqiang Zhong[*]

[*]*The Pennsylvania State University, Department of Aerospace Engineering, University Park, PA 16802*

Abstract. Homogeneous nucleation in supersonic expansions into a near-vacuum is a challenging multiscale problem with many practical applications. This paper discusses the first implementation of classical nucleation theory (CNT) to the direct simulation Monte Carlo modeling of a supersonic jet system. Comparison with experiment highlights the successes as well as limitations of the modeling approach, particularly with respect to the applicability of CNT to unsteady jet expansions. To overcome the main deficiency of CNT, that is, the use of a nucleation rate based on macroscopic thermodynamic properties inappropriate to small clusters, a kinetic nucleation model is proposed. Molecular dynamics is used to assist in the formulation of that model as well as improve the total and inelastic cross section for an Ar gas modeled by the Lennard-Jones interaction.

INTRODUCTION

Cluster formation processes are all encompassing and found in countless applications important to society – medical research, creation of new and novel materials, and developing low cost space-based world wide telecommunications, to name a few. Detailed statistical characterization of cluster properties is important for micro and nano-scale materials fabrication technologies such as chemical vapor deposition, pulsed laser deposition, dry etching, cluster deposition, laser ablation, and growth of nano-tubes. Condensation also plays an important role in the highly complex problem of spacecraft contamination. The original motivation for the Rayleigh scattering measurements of Williams *et al*[1] was to obtain data to develop models to predict spacecraft contamination. Many of the important condensation processes in the above mentioned applications may be studied in free jet expansions which occur when a gas expands from a plenum chamber into a vacuum or a low-pressure background through a small orifice. Since the Knudsen number changes by two and half orders of magnitude, there is no single computational technique that may be used to model this entire flow. The flow closest to the nozzle is continuum, with a typical Knudsen number less than 10^{-3}, hence, the use of DSMC inside this region would be impractical.[2, 3] As the gas expands the translation temperature decreases with distance which creates an environment for the condensation of clusters.[4] The nucleation region is usually in the transitional to rarefied regime, which typically occurs at a distance of a few nozzle diameters from the nozzle exit.[1]

The research presented in this paper discusses the process of cluster formation and evolution in supersonic jets by a multiscale computational model. The model is based on a kinetic particle simulation method, the direct simulation Monte Carlo (DSMC), which is applicable in the transitional to rarefied flow regime. The model is multiscale because, in addition to DSMC, continuum fluid dynamics (CFD)/Navier-Stokes (NS) and molecular dynamics (MD) formulations are also used. The CFD Navier-Stokes approach is used to simulate the initial expansion stage of the dense gas, during which the condensation can be neglected. Molecular dynamics is used primarily to develop a cluster reaction cross section data base for DSMC and to extend the DSMC simulation capabilities further to address issues related to condensation in a dense gas.

[1] The author to whom the correspondence should be addressed, dalevin@psu.edu

MODELING CLUSTER PROCESSES WITH CNT IN DSMC SIMULATIONS OF SUPERSONIC FLOWS

Since the flow is supersonic so that information does not propagate upstream, the usual technique for modeling expanding transitional flows is to use a continuum Navier-Stokes (NS) calculation to the model the dense region closest to the nozzle.[2, 3, 5] When the flow has expanded sufficiently downstream (on the order of a few nozzle radii), the NS solution can be used to generate a starting surface of temperature, velocity, and species concentration macroparameters to begin the DSMC calculation. The steady state numerical solution of the NS equations for laminar, viscous gas expansion can be obtained with a computational tool such as the General Aerodynamics Simulation Program (GASP) which uses a finite spatial discretization.[6] Additional details about the GASP calculations may be found in Ref. [3]

Let us consider the present simulation implementation for an expanding Ar jet with stagnation conditions of 6400 Pa and 170 K, expanding through an orifice with a diameter of 1.4 mm into a vacuum. This corresponds to one of the NS/DSMC simulation cases we have used to test the semi-empirical scaling law predictions for terminal cluster size.[7] Figure 1 shows the Ar gas plume mass density (top) and temperature contours (bottom) obtained by DSMC. The temperature and mass density contours show the general properties of a rapidly expanding gas into a near vacuum background environment. The DSMC numerical parameters are $F_{num} = 8 \times 10^6$, a cluster weighting factor of $W = 5.0 \times 10^{-5}$, and the number of simulated molecules and clusters of $N_m = 0.48 \times 10^6$ and $N_c = 0.34 \times 10^6$, respectively. Similar contours may also be obtained for the near-exit fields generated by the NS solutions. The NS and DSMC calculations are performed on grids that spatially overlap so that a starting surface (shown as dashed lines in Fig. 1) may be generated. The temperature contours seen in Fig. 1 show that there is a smooth connection between the Ar temperature contours obtained with NS/CFD (red) and DSMC (black). This procedure ensures the DSMC solution is independent of the specific starting surface location. The starting surface, typically composed of ~ 500 segments, is constructed from the NS solution for a typical Mach number ≤ 2.5.

In addition to the usual collision processes among the monomers, the processes of cluster formation, growth and decay were incorporated into our DSMC calculations in a manner similar to chemical reactions. The reaction rates used are the CNT rates of cluster nucleation, condensation, and evaporation.[8] Figure 2 shows the average cluster growth along the plume centerline for stagnation conditions of 6400 Pa and various stagnation temperatures.[2] It can be seen that cluster growth weakly depends on the initial conditions, which is consistent with Hagena's derivation of the scaling laws.[7] The small differences between the curves may be attributed to the nonlinear effects of the coupled evaporation and condensation processes accompanying the growth of clusters. In addition, multiple DSMC calculations were performed for different stagnation pressures and orifice diameters. It was found that the initial stagnation condition that produced a terminal cluster size of ~ 500 is a linear function of the orifice diameter.[2, 3] This result demonstrated that the DSMC simulation, using CNT, could predict another of the well known Hagena empirical scaling laws for condensation in argon supersonic jets.[7]

There are two main reasons for why the scaling laws are adequately predicted by CNT. The first is that the flow has a small proportion of clusters, thereby allowing the gas to expand isentropically, an underlying assumption used in the derivation of the scaling laws. The second is that for the particular set of initial conditions considered in the figure, the most typical cluster reactions are the unimolecular type assumed by CNT. In real world applications, the deviations from isentropic conditions will most likely be high and a higher order theory that is computationally tractable is necessary. In fact, our prediction of the cluster size distributions[9] significantly deviates from experimental data.[1] This is consistent with the work of Ohkubo *et al*[10] who also found that the correct prediction of the cluster size distribution along with internal and kinetic energy distributions is beyond the capability of the classic approach.

The reasons for the discrepancy between the CNT-based distributions and experimental data are due to problems inherent with CNT and the flow environment of an expanding jet. The former problems include the ambiguous definition of surface energy of small clusters [11], the negligence of the rotational and translational degrees of freedom of freshly nucleated clusters [12], and the unrealistic description of vapor-cluster and cluster-cluster interactions.[2]

MOVING BEYOND CNT/DSMC - A KINETIC NUCLEATION APPROACH FOR DSMC

A *full* kinetic cluster model for DSMC will involve the development of the appropriate models such as nucleation, evaporation, sticking, cluster-internal energy transfer, and coalescence. Although all are important, our previous work has shown that the spatial and size distribution of clusters in the plume expansion is very dependent on the nucleation model. For this reason, we first investigated a kinetic nucleation approach to replace CNT, and we discuss the high

lights of this research below.[13]

Modeling of Dimer Formation, a Hybrid DSMC-MD Approach

In a kinetic-flowfield scheme one potentially needs to consider a large number of cluster growth and destruction mechanisms specific for each cluster size, clearly an impossible task. To determine the most important nucleation mechanism, a quasi one-dimensional unsteady free expansion was studied by molecular dynamics and it was found that the dominant mechanism to initiate condensation is through dimer formation in a two-stage ternary collision of monomers.[14] To simulate condensation flow with a kinetic nucleation approach, the initial clusters, dimers, have to be created from triple collision processes. Three molecules in a triple collision may collide together as follows,[15]

$$A + A + A \xrightarrow{k_f} A_2 + A \tag{1}$$

where A represents an atom, A_2 represents a stable dimer created from a triple collision and k_f is the forward rate constant for the triple collision process. The probability P_t of creating stable dimers out of triple collisions is related to k_f as[16]

$$n_v k_f = \overline{\sigma c_r} \int_0^\infty P_t(E_t) f\left(\frac{E_t}{kT}\right) d\left(\frac{E_t}{kT}\right) \tag{2}$$

where n_v is the vapor number density, σ is the monomer-monomer collision cross section, c_r is the monomer-monomer collision relative velocity and $f\left(\frac{E_t}{kT}\right)$ is the collision energy distribution function. There are two reasons that we can not directly apply the above model in this work. First the triple collision forward rate constant is strongly dependent on the vapor environment and is not available from the literature for the Argon case studied in this work. Secondly, the DSMC approach is developed to deal with binary collisions. Hence, the triple collision process, shown in Eq. (1), has to be modified in a DSMC scheme. To avoid these difficulties, the triple collision shown in Eq. (1) is decomposed into two successive binary collision steps as[17]

$$A + A \rightarrow A_2^* \tag{3}$$

and

$$A_2^* + A \rightarrow A_2 + A \tag{4}$$

The atom-atom binary collision (A-A) generates a temporary pair A_2^* with a lifetime which is approximately equal to a binary collision duration. The pair A_2^*, known as a collision complex, may collide with a third monomer during its lifetime to create a stable dimer, as indicated as Eq. (4).

It is well known that the number of atom-atom collision pairs is proportional to N^2, where N is the number of simulated particles. To decrease the computational cost, the No Time Counter (NTC)[18] and Majorant Frequency (MF)[19] schemes have been developed to numerically decrease the number of collision pairs, while increasing the probability for an accepted collision. In this work, we use the DSMC-based SMILE[19] code which uses the MF scheme for selecting collision pairs. The majorant collision frequency ν is given by,

$$\nu = (N_c(N_c - 1)/2) \{\sigma(v)v\}_{max} \tag{5}$$

where N_c is the number of molecules in a cell, $\sigma(v)$ is the total collision cross section, and v is the collision relative velocity. The collision probability for collision pairs calculated from Eq. (5) is

$$\frac{\sigma(v)v}{\{\sigma(v)v\}_{max}} \tag{6}$$

The procedure of modeling the triple collision in two separate steps in a DSMC scheme can be summarized as follows. The number of atom-atom collision pairs is calculated using the original DSMC scheme, Eq. (5). For an accepted atom-atom collision pair, defined as a collision complex A_2^*, the number of A_2^*-atom collision pairs is further calculated during the A_2^* lifetime. Note that the center of mass velocity of the atom-atom collision pair is assumed to be the A_2^* velocity and the value of $\sigma(v)$ in Eq. (6) is assumed to be constant and equal to $\sigma(v) = \frac{\pi}{4}\left(\frac{d_* + d_0}{2}\right)^2$. As in the traditional DSMC method, the acceptance-rejection principle is used to evaluate whether the A_2^*-atom collision,

referred as the triple collision in this work, occurs or not. For a successful triple collision, if the selected random number is less than the probability P_t, a dimer would be created and at the same time two atoms out of the initial three colliding atoms would be consumed. The probability P_t is defined as the ratio of the number of stable dimers to total number of A_2^*-atom collisions. The A_2^* lifetime and the probability P_t are obtained as follows.

To obtain the complex lifetime, the molecular dynamics (MD) method is chosen to simulate various binary collision processes corresponding to the initial conditions that will ultimately be needed in the DSMC simulations. The intermolecular force between Argon atoms is calculated from the 6-12 Lennard-Jones potential with a well depth σ of 3.405 Å and ε of 0.0103 eV. A time step of 1.0×10^{-15} is used in the MD simulation. In a typical simulation case, two molecules first move freely toward each other, then collide at some range, and finally separate beyond a range where they have any interaction. The beginning and end of a collision are determined by the times at which the particle velocity starts or stops changing. Thus, a collision duration, assumed to be the A_2^* lifetime, is able to be calculated from the results of the MD trajectory simulations.

The MD simulation results of a binary collision duration for Argon atoms are shown in Fig. 3 as a function of typical collision relative velocity and impact parameter. The collision duration time is regarded as the lifetime of the Argon complex A_2^*. Each symbol in Fig. 3 represents one simulation case. It can be seen that, for the collisions with the same relative velocity, the duration time increases as the impact parameter increases. The duration time reaches a maximum value at a critical impact parameter, R, then it quickly decreases to zero for the collisions with impact parameters larger than the critical value. For the collisions with the same impact parameter, Fig. 3 shows that the duration time decreases as the relative velocity increases.

For a single relative kinetic energy, an average collision duration, τ, can be calculated from Fig. 3 based on an R^2 distribution of collision pairs as follows,

$$\tau = \frac{1}{R^2} \int_{r=0}^{r=R} \tau(r)\, dr^2 \tag{7}$$

where R is the radius of the collision cross section, and $\tau(r)$ is a collision duration time of the collision with an impact parameter of r. The value of R is seen from Fig. 3 to be a function of the collision relative velocity and was chosen as the impact parameter corresponding to maximum collision duration time in each case.

The average collision duration obtained from the MD simulations, compared with lifetimes calculated by Bunker's approximate formula,[15] are shown in Fig. 4. Bunker's formula, derived for particles that interact by the attractive part of the Lennard-Jones potential, provides the following relationship between the mean collision duration time τ, the parameters of the interaction potential ε and σ, the reduced mass μ, and the relative translational energy E_t:

$$\tau \approx \frac{3}{2} \sigma \mu^{\frac{1}{2}} \varepsilon^{\frac{1}{6}} E_t^{-\frac{2}{3}} \tag{8}$$

We can see in Fig. 4 that Bunker formula poorly describes the actual MD results indicated as the triangular symbols. Another recent MD study[17] has also shown that actual mean collision duration significantly deviates from Eq. (8). As a first step we use a constant value of $\tau = 10$ psec corresponding to a relative velocity of $\sim$100 m/s which is a typical condition in the expanding plume flow.

The probability P_t to form a stable dimer is defined as the ratio of the number of stable dimers, N_d, to the number of triple collisions, N_t,

$$P_t = \frac{N_d}{N_t} \tag{9}$$

The probability P_t may be computed directly from MD simulations by tracing each molecular position, momentum and energy, and counting the number of triple collisions and stable dimers based on a geometric criteria[20] and history tracking method.[14] The MD system may consist of only three molecules and simulation results are averaged over many repeated cases, or a large MD system is simulated and the results are sampled over a period of time. To separate the dimers from the colliding pairs in a MD system, two particles are only regarded as a stable dimer on the condition that their interaction time is longer than the binary collision duration.[14] In this way, the number of dimers can be counted in a MD system.

To count the number of triple collisions in a MD system, the relative distance among simulated particles needs to be calculated continuously to determine whether a triple collision has occurred. Due to a high computational cost, it may be challenging to separate triple collisions from the dimer-monomer collisions in the MD simulation. Instead a DSMC simulation may be used to count the number of triple collisions, N_t. In our DSMC simulations, the original collision scheme shown in Eq. (5) is used to calculate the number of A_2^*-atom triple collision "pairs" during the complex lifetime

and the probability, calculated by Eq. (6), is used to determine whether the collision pairs are accepted or refused. The computational details of the hybrid MD-DSMC method used to calculate P_t may be found in Ref. [13]. The values of P_t were found to be not sensitive to the degree of supersaturation and a constant probability of 0.217 of was used in the full DSMC simulations.[13]

Results and Discussions

Here we consider condensation in a free expanding pure Argon plume through a sonic nozzle with a stagnation pressure of 125 torr, a stagnation temperature of 280 K, and orifice diameter of 3.2 mm. The details of DSMC simulation numerical parameters may be found in Ref. [13]. Figure 5 compares the cluster number density contours in the condensation plume for the simulations using the kinetic (top) and CNT (bottom) nucleation models. It can be seen that the cluster number density contours for the simulation using CNT have much higher fluctuations than the contours obtained from the kinetic nucleation process. This is because in the kinetic model the initial clusters are created through a modified standard DSMC collision processes, while the distribution of initial clusters for the simulation using CNT is highly sensitive to the vapor environment characteristics such as the degree of supersaturation S and vapor temperature T. Note that even using larger numbers of simulated particles and samples, there is no significant improvement in the degree of fluctuations in the CNT simulations. Figure 5 shows that the cluster number density obtained from the kinetic nucleation process is about three to four orders of magnitude larger than that from CNT.

Figure 6 compares contours of the average cluster size between the kinetic (top) and CNT (bottom) nucleation models. It can be seen that the average cluster size obtained from the kinetic nucleation process is smaller than the value obtained from the CNT nucleation process. The outcome of Argon cluster-monomer collisions[3] can be described by average sticking probabilities as a function of cluster size, as shown in Fig. 7. According to these values, the average sticking probability for a cluster size less than 11-mers increases quickly as the cluster size increases, while for cluster size larger than 10-mers, the sticking probability is very close to unity. The initial dimers generated in the kinetic nucleation process are difficult to grow through the dimer-monomer collision processes due to a small probability around 0.05. However, the CNT nucleation process defines the critical clusters as the initial clusters, and the critical clusters can stick with the colliding monomers quickly due to a large probability close to unity. Since large number of small clusters exist for the simulation using the kinetic nucleation process, its average cluster size can be less than one-tenth than the corresponding value obtained for the simulation using the CNT nucleation theory.

To quantitatively compare the kinetic and CNT nucleation process results, Fig. 8 shows the distributions of cluster number density and cluster size along the plume centerline. It can be seen from Fig. 8 that the initial clusters, dimers, in the kinetic nucleation process appear earlier than the initial critical clusters in the CNT simulation. The maximum cluster number density on the centerline shown in the kinetic nucleation simulation is at a position downstream of the location shown for the CNT simulation. For the simulation using the kinetic nucleation process, the maximum cluster number density on the centerline is about $8.0 \times 10^{+20}$ per m^3 at the axial distance of 0.01m downstream of the nozzle exit, while the CNT nucleation predicts the maximum cluster number density is about $3.0 \times 10^{+17}$ at the axial distance of 0.007 m. One possible reason is that the CNT neglects transient nuclei formation time[21] which would affect the generation location of nuclei in a supersaturated vapor environment. Due to a larger cluster number density and smaller initial cluster size, the cluster growth process is slower in the simulation using the kinetic nucleation process than the CNT nucleation process. At an axial position of 0.032m, 10 nozzle throat diameters downstream from the nozzle exit, the average cluster size consists of approximately 950 molecules in the CNT simulation and 50 molecules in the kinetic simulation, while the cluster number density is about $2.72 \times 10^{+16}$ per m^3 in the CNT simulation and $8.70 \times 10^{+19}$ in the kinetic simulation. Thus, it can be seen that the condensation results are quite different for the simulations using the kinetic and CNT nucleation processes.

Based on the numerical results, we may conclude that the CNT theory estimates the nucleation rate 3-4 orders of magnitude less than the kinetic nucleation model does for homogeneous condensation in a free expanding Argon plume. The fundamental difference between these two nucleation models is that CNT neglects the large number of small clusters which potentially can also grow to large clusters even though the small sticking collision probabilities for dimers are lower than those for large clusters. Since the existence of small clusters affects the cluster number density and average cluster size, it is important to use the kinetic nucleation model to accurately simulate a homogeneous condensation flow. Moreover, the semi-empirical relationship of Knuth[22] strongly suggests that there is a terminal dimer mole fraction of approximately 1%, whereas, CNT would predict it to be nonexistent.

ACKNOWLEDGMENTS

The research performed at the Pennsylvania State University was supported by the Air Force Office of Scientific Research Grant No. F49620-02-1-0104 and the National Science Foundation Grant No. CTS-0521968 whose support is gratefully acknowledged.

REFERENCES

1. Williams, W., and Lewis, J., *Arnold Engineering Development Center* (1980).
2. Zhong, J., Gimelshein, S. F., Zeifman, M. I., and Levin, D. A., *AIAA Paper 2004-0166* (2004).
3. Zhong, J., Gimelshein, S. F., Zeifman, M. I., and Levin, D. A., *AIAA Journal*, **43**, 1781–1796 (2005).
4. Haberland, H., *in Clusters of Atoms and Molecules, edited by H. Haberland (Springer, Berlin)*, p. 207 (1994).
5. Gimelshein, S., Levin, D., and Alexeenko, A., *J. Spacecraft Rockets* (accepted for publication, 07 Jul 2003).
6. *The General Aerodynamic Simulation Program, GASP*, Aerosoft, Inc., Virginia, version 4.1 edn. (2004), computational Flow Analysis Software for the Scientist and Engineer, User's Manual.
7. Hagena, O. F., and Obert, W., *J. Chem. Phys.*, **56**, 1793 (1972).
8. Abraham, F., *Homogeneous Nucleation Theory: The Pretransition Theory of Vapor Condensation*, Academic Press, New York, 1974.
9. Zhong, J., Zeifman, M. I., and Levin, D. A., *Journal of Thermophysics and Heat Transfer*, **20**, 41–51 (2005).
10. Ohkubo, T., Kuwata, M., Luk'yanchuk, B., and Yabe, T., *Appl. Phys.*, **A 77**, 271 (2003).
11. McDonald, J. E., *Am. J. Phys.*, **31**, 31 (1963).
12. Sharaf, M., and Dobbins, R., *J. Chem. Phys.*, **77**, 1517 (1982), and references therein.
13. Zhong, J., Gratiy, S., Zeifman, M., and Levin, D., *AIAA Paper No. 2005-2950.* (2005).
14. Zhong, J., Zeifman, M. I., and Levin, D. A., *Physics of Fluids*, **17**, 128102 (2005).
15. Bunker, D. L., *J. Chem. Phys.*, **32**, 1001–1005 (1960).
16. Boyd, I. D., *Physics of Fluids A*, **4**, 178–185 (1992).
17. Bunker, D. L., Bernshtein, V., and Oref, I., *J. Phys. Chem. A*, **105**, 3454–3457 (2001).
18. Bird, G. A., *Molecular Gas Dynamics and the Direct Simulation of Gas Flows*, Clarendon Press, Oxford, 1994.
19. Ivanov, M. S., Markelov, G. N., and Gimelshein, S. F., *AIAA Paper 1998-2669* (1998).
20. Soto, R., and Cordero, P., *J. Chem. Phys.*, **110**, 7316–7325 (1999).
21. Wu, D. T., *J. Chem. Phys.*, **97**, 2644–2650 (1992).
22. Knuth, E., *Journal of Chemical Physics*, **66**, 3515–3525 (1977).

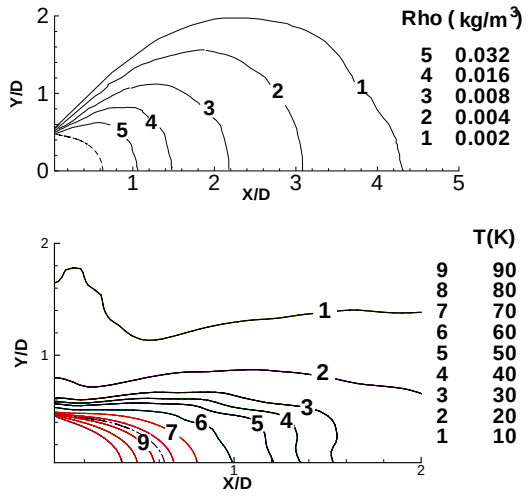

FIGURE 1. Argon gas mass density (kg/m^3) contours (top) and temperature (K) contours (bottom) for an Argon gas jet expansion obtained from a DSMC simulation.

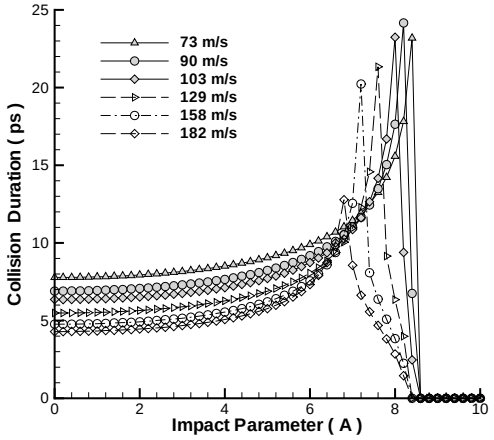

FIGURE 3. MD trajectory studies of the binary collision duration as a function of the impact parameter and the collision relative velocity.

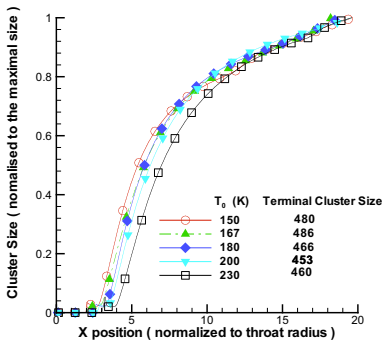

FIGURE 2. Argon cluster growth along the centerline of the DSMC simulation for an orifice diameter of 0.14 mm.

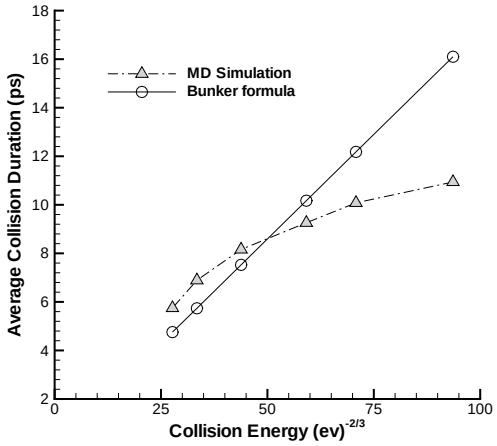

FIGURE 4. Comparison between MD and the Bunker formula of average collision duration for different relative collision energies.

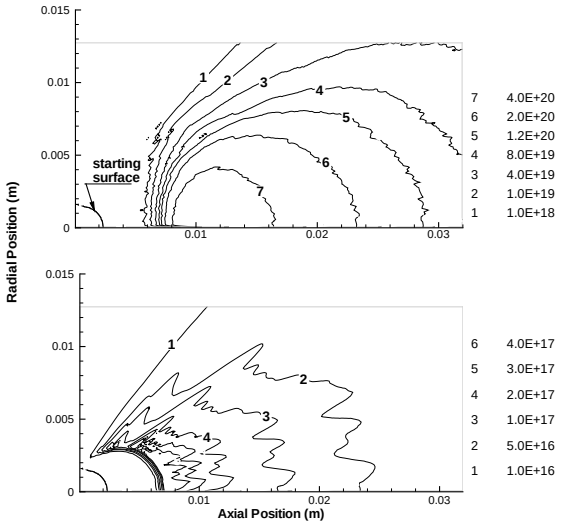

FIGURE 5. Comparison of average cluster number density contours (m^{-3}) in a free expanding condensation Argon plume between the kinetic (top) and CNT (bottom) nucleation models.

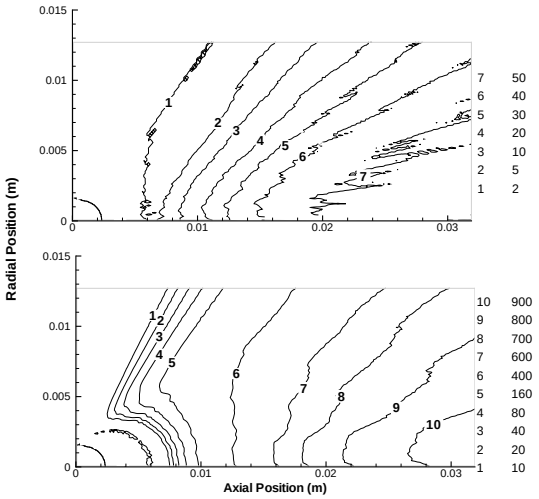

FIGURE 6. Comparison of average cluster size (number of monomers) contours in a free expanding condensation Argon plume between the kinetic (top) and CNT (bottom) nucleation models.

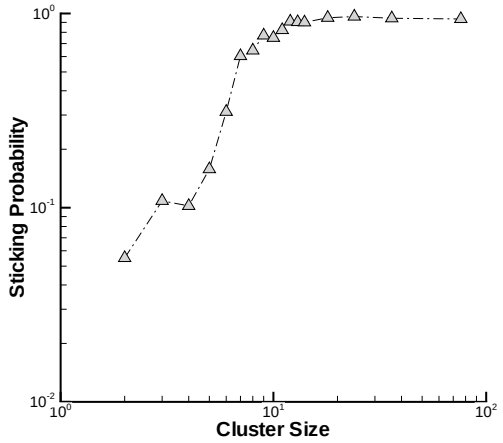

FIGURE 7. Average Argon cluster-monomer sticking probabilities from Ref. 12

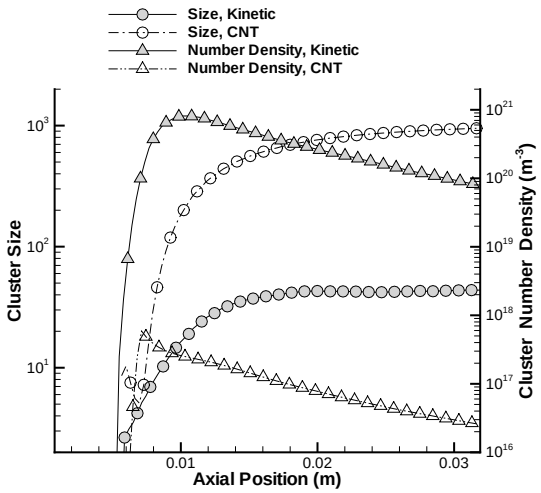

FIGURE 8. Comparison of average cluster size and number density along the plume centerline between the kinetic and CNT nucleation models.